

String Interactions in PP-wave from $\mathcal{N} = 4$ Super Yang Mills

Min-xin Huang *

*David Rittenhouse Laboratories, University of Pennsylvania
Philadelphia, PA 19104, U.S.A.*

Abstract

We consider non-planar contributions to the correlation functions of BMN operators in free $\mathcal{N} = 4$ super Yang Mills theory. We recalculate these non-planar contributions from a different kind of diagram and find some exact agreements. The vertices of these diagrams are represented by free planar three point functions, thus our calculations provide some interesting identities for correlation functions of BMN operators in $\mathcal{N} = 4$ super Yang Mills theory. These diagrams look very much like loop diagrams in a second quantized string field theory, thus these identities could possibly be interpreted as natural consequences of the pp-wave/CFT correspondence.¹

1 Introduction

The AdS/CFT correspondence states that the $\mathcal{N} = 4$ SU(N) Yang-Mills theory is equivalent to IIB string theory quantized on the $AdS_5 \times S^5$ background [1]. Recently Berenstein, Maldacena and Nastase [2] have argued that IIB superstring theory on a pp-wave background with Ramond-Ramond flux is dual to a sector of $\mathcal{N} = 4$ SU(N) super Yang-Mills theory containing operators with large R-charge J . The pp-wave solution of type IIB supergravity has 32 supersymmetries and can be obtained as a Penrose limit of $AdS_5 \times S^5$ [3]. While the application of the AdS/CFT correspondence in the usual $AdS \times S$ background is difficult to go beyond the supergravity approximation on the string theory side, the string worldsheet theory in the pp-wave background is exactly solvable, as shown by [4]. More recently, there have been some progress on the question of string interactions [5]-[17].

*minxin@sas.upenn.edu

¹For convenience we will call these diagrams "string theory diagram", although there are reasonable doubts whether these calculations are truly string theory calculations since it is not known how to compute general loop amplitudes in a second quantized string theory. (see a recent paper [28] for progress in this direction.)

It is pointed out in [5, 6, 8] that in BMN limit some non-planar diagrams of arbitrary genus survive and string interactions in pp-wave involve two expansion parameters

$$\lambda' = \frac{g_{YM}^2 N}{J^2} = \frac{1}{(\mu p^+ \alpha')^2} \quad (1)$$

$$g_2 = \frac{J^2}{N} = 4\pi g_s (\mu p^+ \alpha')^2 \quad (2)$$

Here the expansion in g_2 comes from non-planar diagrams. There are operator mixings in this limit. The BMN operators no longer have well defined conformal dimensions and need to be redefined order by order [5, 8].² In this paper for simplicity we will only consider free Yang Mills theory, i.e. we set $\lambda' = 0$, so the only expansion parameter is g_2 . Also there will be no anomalous conformal dimensions in this case and we do not need to consider operator mixing.

It is proposed in [8] that the interaction amplitude for a single string to split into two strings (or two strings joining into one string) is related to the three point function of the corresponding operators in the dual CFT. Using this relation the authors in [8] are able to compute the second order correction to the anomalous dimension of the BMN operator from free planar three point functions and found exact agreement with computation of the field theory torus contributions to the two point function. All calculations in [8] were done in the field theory side but has a clear interpretation from dual string theory. This proposal has been explicitly checked [12, 13, 14, 15, 10] by calculations from light cone string field theory in pp-wave [9].³

It has been pointed out that in type IIB light cone string field theory string interactions should contain quartic or higher order contact interactions in addition to cubic interactions [24], but for some unknown reasons in pp-wave we only need to consider cubic vertex, representing string joining and splitting. This is justified by our calculations where we find precise agreements by only including cubic vertices. Similar point of view is also taken in a recent paper [16] (see figure 1). It would be interesting if higher order interactions indeed vanish in pp-wave light cone string field theory and we leave it for future works. In this paper we will represent the vertices in string theory diagrams with free planar three point functions according to the proposal of [8].⁴ Some free planar three point functions involving BMN operators

²It has been argued earlier that non-planar contributions to large charge operator correlators are important [18] [19]. Here in the BMN limit the R-charge goes like $J \sim N^{\frac{1}{2}}$ and the non-planar diagrams are perturbative in the expansion parameter g_2 . If the R-charge is larger, non-planar diagrams will dominate over planar diagrams [18], and the strings blow up into giant gravitons by Myers effect [20, 21]. Giant gravitons are D3 branes described by determinants and subdeterminants instead of trace operators in CFT [18]. Open strings attached to giant gravitons are described in [22].

³Another interesting approach to this question is to use matrix string theory [23], see [11].

⁴The matrix element in [8] contain a prefactor and a vertex, but for some unknown reasons we do not need to use the prefactor. We leave the explanation to future works.

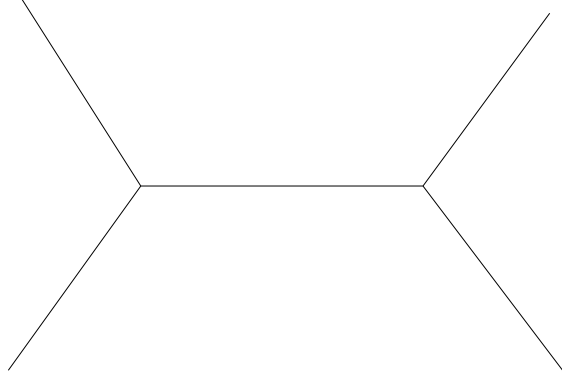


Figure 1: It is recently pointed out in [16] that higher point string interactions in pp-wave can be reduced to cubic interactions under some double pinching limits. For example, the skeleton diagram with s , t and u channels appear in the computation of a planar four point function $\langle \bar{O}_1 \bar{O}_2 O_3 O_4 \rangle$ as we take some specific double pinching limits. We will only need to consider cubic interactions in our calculations of the string theory diagram.

have been computed in [8]. Specifically, we have (Assuming $m \neq 0$ and $n \neq 0$)

$$\langle \bar{O}^J O^{J_1} O^{J_2} \rangle = \frac{g_2}{\sqrt{J}} \sqrt{x(1-x)} \quad (3)$$

$$\langle \bar{O}_0^J O^{J_1} O_0^{J_2} \rangle = \frac{g_2}{\sqrt{J}} x^{\frac{1}{2}} (1-x) \quad (4)$$

$$\langle \bar{O}_{00}^J O_0^{J_1} O_0^{J_2} \rangle = \frac{g_2}{\sqrt{J}} x(1-x) \quad (5)$$

$$\langle \bar{O}_{m,-m}^J O_0^{J_1} O_0^{J_2} \rangle = -\frac{g_2}{\sqrt{J}} \frac{\sin^2(\pi m x)}{\pi^2 m^2} \quad (6)$$

$$\langle \bar{O}_{00}^J O_{00}^{J_1} O^{J_2} \rangle = \frac{g_2}{\sqrt{J}} x^{\frac{3}{2}} \sqrt{1-x} \quad (7)$$

$$\langle \bar{O}_{m,-m}^J O_{n,-n}^{J_1} O^{J_2} \rangle = \frac{g_2}{\sqrt{J}} x^{\frac{3}{2}} \sqrt{1-x} \frac{\sin^2(\pi m x)}{\pi^2 (m x - n)^2} \quad (8)$$

$$\langle \bar{O}_{00}^J O_{n,-n}^{J_1} O^{J_2} \rangle = 0 \quad (9)$$

where $x = J_1/J$ and $J = J_1 + J_2$. Note the spacetime dependences of two point and three point functions in conformal field theory are determined by conformal symmetry. Here and elsewhere in this paper we have omitted the factors of spacetime dependence in the correlators. The definition of the properly normalized chiral and BMN operators are

$$O^J = \frac{1}{\sqrt{N^J J}} \text{Tr} Z^J \quad (10)$$

$$O_0^{J_1} = \frac{1}{\sqrt{N^{J_1+1}}} \text{Tr}(\phi^{I_1} Z^{J_1}) \quad (11)$$

$$O_0^{J_2} = \frac{1}{\sqrt{N^{J_2+1}}} \text{Tr}(\phi^{I_2} Z^{J_2}) \quad (12)$$

$$O_{m,-m}^J = \frac{1}{\sqrt{JN^{J+2}}} \sum_{l=0}^J e^{2\pi i m l / J} \text{Tr}(\phi^{I_1} Z^l \phi^{I_2} Z^{J-l}). \quad (13)$$

Here ϕ^{I_1} and ϕ^{I_2} represent excitations in two of the eight transverse directions.

The proposal of this paper is that we can calculate non-planar contributions to BMN correlation functions in free Yang Mills theory from string theory point of view. The details of how to do the calculation will be clear from our specific examples. Some non-planar contributions to the two point and three point functions of BMN operators have been computed on the field theory side in [5, 8]. For example, the free torus (genus one) two functions of BMN operators are

$$\begin{aligned} & \langle \bar{O}_{n,-n}^J O_{m,-m}^J \rangle_{\text{torus}} \quad (14) \\ &= \frac{g_2^2}{24}, \quad m = n = 0; \\ &= 0, \quad m = 0, n \neq 0 \text{ or } n = 0, m \neq 0; \\ &= g_2^2 \left(\frac{1}{60} - \frac{1}{24\pi^2 m^2} + \frac{7}{16\pi^4 m^4} \right), \quad m = n \neq 0; \\ &= \frac{g_2^2}{16\pi^2 m^2} \left(\frac{1}{3} + \frac{35}{8\pi^2 m^2} \right), \quad m = -n \neq 0; \\ &= \frac{g_2^2}{4\pi^2 (m-n)^2} \left(\frac{1}{3} + \frac{1}{\pi^2 n^2} + \frac{1}{\pi^2 m^2} - \frac{3}{2\pi^2 m n} - \frac{1}{2\pi^2 (m-n)^2} \right), \text{ all other cases} \end{aligned}$$

The paper is organized as follows. In section 2 we reproduce equation (14) from one loop string propagation diagram calculation. In section 3 we calculate the torus contribution to a three point function involving BMN operators both in field theory side and in string theory side. We also find nontrivial agreements in this case. In section 4 and appendix B we do more calculations giving more evidences of our proposal.

2 One loop string propagation

We consider a single string propagating in the pp-wave background. We expect the one loop correction to the string propagation to be the torus contribution to the two

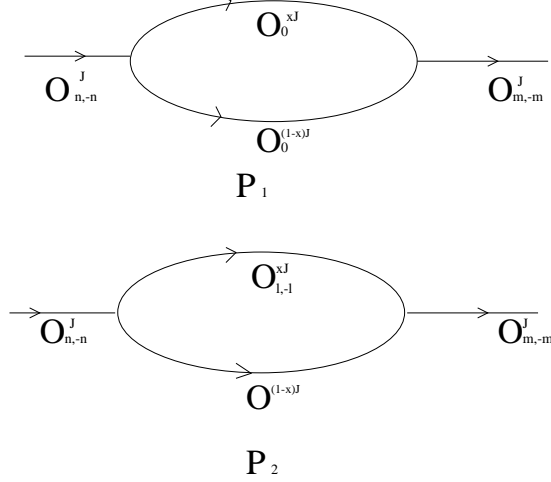


Figure 2: There are 2 diagrams contributing the one loop string propagation. The BMN string $O_{n,-n}^J$ can split into two strings $O_{l,-l}^{J_1}$, O^{J_2} or $O_0^{J_1}$, $O_0^{J_2}$ and joining back into another string $O_{m,-m}^J$. We denote contributions to these two diagrams P_1 and P_2 .

point function of corresponding BMN operators. On the other hand, the one loop amplitude can be calculated by summing over the amplitudes of the string splitting into two strings and then joining back into a single string. The cubic vertices of string splitting and joining can be represented by free planar three point functions. There are two diagrams associated with this process as shown in figure 2. The BMN string $O_{n,-n}^J$ can split into two strings $O_{l,-l}^{J_1}$, O^{J_2} or $O_0^{J_1}$, $O_0^{J_2}$ and joining back into another string $O_{m,-m}^J$. We denote the contributions from these two processes by P_1 and P_2 . Then

$$\begin{aligned}
P_1 &= \sum_{J_1=0}^J \langle \bar{O}_{n,-n}^J O_0^{J_1} O_0^{J_2} \rangle_{planar} \langle \bar{O}_0^{J_1} \bar{O}_0^{J_2} O_{m,-m}^J \rangle_{planar} \\
&= g_2^2 \int_0^1 dx \frac{\sin^2(m\pi x)}{m^2 \pi^2} \frac{\sin^2(n\pi x)}{n^2 \pi^2}
\end{aligned} \tag{15}$$

$$\begin{aligned}
P_2 &= \sum_{J_1=0}^J \sum_{l=-\infty}^{+\infty} \langle \bar{O}_{n,-n}^J O_{l,-l}^{J_1} O^{J_2} \rangle_{planar} \langle \bar{O}_{l,-l}^{J_1} \bar{O}^{J_2} O_{m,-m}^J \rangle_{planar} \\
&= g_2^2 \sum_{l=-\infty}^{+\infty} \int_0^1 dx x^3 (1-x) \frac{\sin^2(m\pi x)}{\pi^2 (mx-l)^2} \frac{\sin^2(n\pi x)}{\pi^2 (nx-l)^2}
\end{aligned} \tag{16}$$

The string theory diagrams are computed by multiplying all vertices and summing over all possible intermediate operators. Here we do not need to use propagators

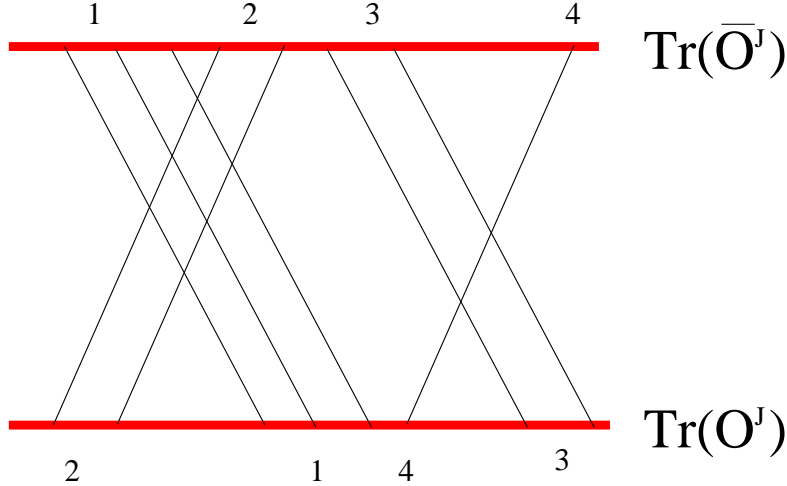


Figure 3: Feymann diagram of torus contraction of large N gauge indices [5, 8]. We are contracting non-planarly by dividing the string into 4 segments.

in calculating the diagrams. In large J limit we can approximate the sum in J_1 by a integral $\sum_{J_1=0}^J = J \int_0^1 dx$. It is straightforward to put equations (3) to (9) into equations (15) (16) and explicitly compute the sum and integral. We find an agreement with equation (14) in all 5 cases

$$\langle \bar{O}_{n,-n}^J O_{m,-m}^J \rangle_{torus} = \frac{1}{2}(P_1 + P_2) \quad (17)$$

Here the $\frac{1}{2}$ can be thought of as the symmetry factor of the string theory diagrams. The symmetry factor can be understood from the example of free torus two point function of chiral operators, which is computed in the field theory side as shown in figure 3 [5, 8]. The twistings in the large N gauge index contractions can be thought of intuitively as string splitting and rejoining. In appendix A we give an argument why we have overcounted by a factor of 2 when we do string theory diagrams. In more general cases of one loop cubic interaction and two loop propagation diagrams the symmetry factors will be determined by more complicated combinatorics and will generally differ from the symmetry factors in usual Feymann diagrams in quantum field theory. In appendix A we derive the symmetry factors of one loop cubic diagrams and find agreements with direct calculations of field theory and string theory diagrams. We have not determined the symmetry factors for two loop propagation diagrams. Nevertheless we can still do some interesting calculations in section 4 and appendix B without knowing the symmetry factors.

One can also easily calculate the one loop string propagation diagram for chiral operators O^J and O_0^J . In both cases there is only one diagram. The results are again agree with the field theory calculations by the symmetry factor of $\frac{1}{2}$.

3 One loop cubic string interaction

3.1 Free torus three point functions of BMN operators

The non-planar contributions to the three point functions of large charge chiral operators have been computed to arbitrary genus using Gaussian matrix model [5]. Here we calculate the torus three point functions using gauge theory Feymann diagram and generalize calculations to BMN operators. The calculations in this subsection follow very closely as in [5, 8]. First we consider three point function of chiral operators $\langle \bar{O}^J O^{J_1} O^{J_2} \rangle$. There are 3 types of torus diagrams as shown in Figure 4. We denote the contributions from these 3 diagrams Q_1 , Q_2 and Q_3 . We can see Q_1 is to divide one of the small operators into 5 groups, so we have a factor of $\frac{1}{4!}$. Q_2 is to divide one of the small operators into 4 groups and the other one into 2 groups, so we have a factor of $\frac{1}{3!1!}$. Q_3 is to divide both small operators into 3 group, so the factor is $\frac{1}{2!2!}$. We caution the reader here we have overcounted by a factor of 2 in Q_2 and a factor of 3 in Q_3 by cyclicity. The final answer is

$$Q_1 = \frac{1}{24} \frac{g_2^3}{\sqrt{J}} \sqrt{x(1-x)} [x^4 + (1-x)^4] \quad (18)$$

$$Q_2 = \frac{1}{12} \frac{g_2^3}{\sqrt{J}} \sqrt{x(1-x)} [x^3(1-x) + x(1-x)^3] \quad (19)$$

$$Q_3 = \frac{1}{12} \frac{g_2^3}{\sqrt{J}} \sqrt{x(1-x)} [x^2(1-x)^2] \quad (20)$$

Here again $x = J_1/J$. One can easily check this calculation by expand to the first order the three point function equation (3.4) in [5].

Now we consider the three point function involving BMN operator $\langle \bar{O}_{m,-m}^J O_0^{J_1} O_0^{J_2} \rangle$. The calculation is to insert two scalars in the diagrams in Figure 4 and sum over all positions with phases [5, 8]. We denote contributions from the 3 diagrams Q'_1 , Q'_2 and Q'_3 , then

$$Q'_1 = \frac{g_2^3}{\sqrt{J}} \int_0^1 dj_1 dj_2 dj_3 dj_4 dj_5 dj_6 \delta(j_1 + j_2 + j_3 + j_4 + j_5 - x) \delta(j_6 - (1-x)) \int_0^x dy_1 e^{2\pi i m y_1} \int_x^1 dy_2 e^{-2\pi i m y_2} + (x \rightarrow (1-x)) \quad (21)$$

$$Q'_2 = \frac{1}{2} \frac{g_2^3}{\sqrt{J}} \int_0^1 dj_1 dj_2 dj_3 dj_4 dj_5 dj_6 \delta(j_1 + j_2 + j_4 + j_5 - x) \delta(j_3 + j_6 - (1-x)) \left(\int_0^{j_1+j_2} + \int_{j_1+j_2+J_3}^{j_1+j_2+j_3+j_4+j_5} \right) e^{2\pi i m y_1} dy_1 \left(\int_{j_1+j_2}^{j_1+j_2+j_3} + \int_{j_1+j_2+j_3+j_4+j_5}^1 \right) e^{-2\pi i m y_2} dy_2 + (x \rightarrow (1-x)) \quad (22)$$

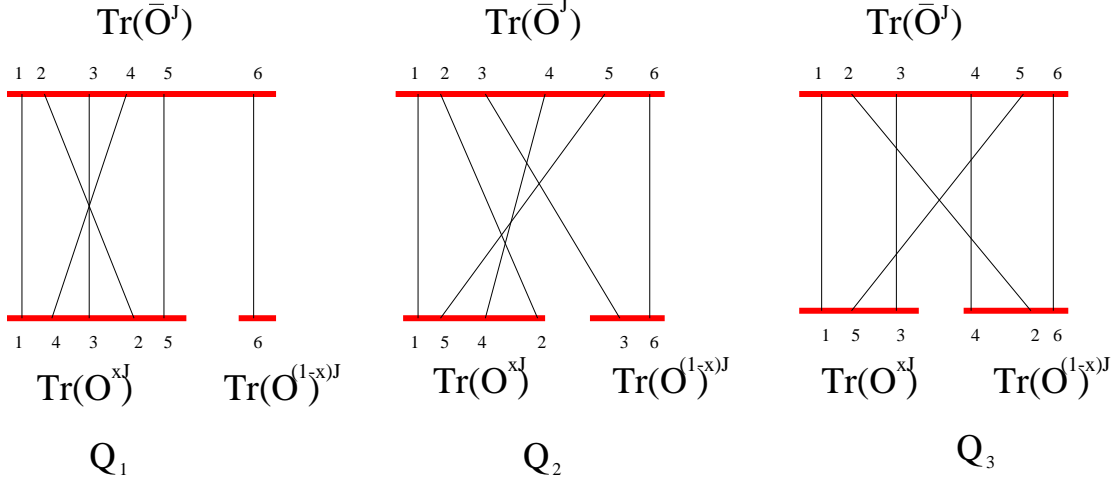


Figure 4: There are three diagrams contribute to the torus three point function. We denote their contributions by Q_1 , Q_2 and Q_3 . Here we use single line notation. One would check these diagrams indeed have a power of $1/N^3$ in double line notation. The top line and the bottom lines represent the long string and short strings. In the three diagrams we have divided the long string into 6 groups and the short strings into (5,1), (4,2) and (3,3) groups. Each group is represented by a single line here.

$$\begin{aligned}
Q'_3 &= \frac{1}{3} \frac{g_2^3}{\sqrt{J}} \int_0^1 dj_1 dj_2 dj_3 dj_4 dj_5 dj_6 \delta(j_1 + j_3 + j_5 - x) \delta(j_2 + j_4 + j_6 - (1-x)) \\
&\quad \left(\int_0^{j_1} + \int_{j_1+j_2}^{j_1+j_2+j_3} + \int_{j_1+j_2+j_3+j_4}^{j_1+j_2+j_3+j_4+j_5} \right) e^{2\pi i m y_1} dy_1 \\
&\quad \left(\int_{j_1}^{j_1+j_2} + \int_{j_1+j_2+j_3}^{j_1+j_2+j_3+j_4} + \int_{j_1+j_2+j_3+j_4+j_5}^1 \right) e^{-2\pi i m y_2} dy_2
\end{aligned} \tag{23}$$

Calculations of these integrals give

$$Q'_1 = \frac{g_2^3}{\sqrt{J}} \frac{1}{24} \left(-\frac{\sin^2(m\pi x)}{m^2 \pi^2} \right) (x^4 + (1-x)^4) \tag{24}$$

$$\begin{aligned}
Q'_2 &= \frac{g_2^3}{\sqrt{J}} \frac{1}{24 m^6 \pi^6} [3 - 3m^2 \pi^2 x(1-x) - 2m^4 \pi^4 (1-x)x^3 \\
&\quad + (-3 - 3x(1-x)m^2 \pi^2) \cos(2m\pi x) + (3(1-2x)m\pi - m^3 \pi^3 x^3) \sin(2m\pi x)] \\
&\quad + (x \rightarrow (1-x))
\end{aligned} \tag{25}$$

$$\begin{aligned}
Q'_3 &= \frac{g_2^3}{\sqrt{J}} \frac{1}{16 m^6 \pi^6} [- (3 + (-1 - 2x + 2x^2)m^2 \pi^2 + 2x^2(1-x)^2 m^4 \pi^4) \\
&\quad + (3 - (1-2x)^2 m^2 \pi^2) \cos(2m\pi x) - 3(1-2x)m\pi \sin(2m\pi x)]
\end{aligned} \tag{26}$$

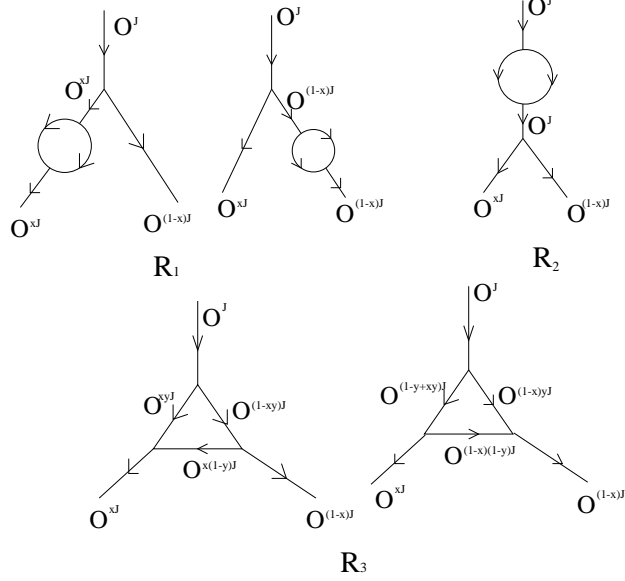


Figure 5: String theory diagrams contribute to $\langle \bar{O}^J O^{J_1} O^{J_2} \rangle_{torus}$ organized in 3 groups. Diagrams in R_1 and R_2 are corrections to one particle propagator while diagrams R_3 are amputated. The two diagrams in R_3 are symmetric by exchange of the two decayed operators.

3.2 String theory loop diagram calculations

First we consider the simple case of one loop diagrams of chiral operators $\langle \bar{O}^J O^{J_1} O^{J_2} \rangle_{torus}$. The diagrams are depicted in figure 5. We classify the diagrams into three groups and denote their contributions R_1 , R_2 and R_3 . R_1 and R_2 are propagator corrections to planar three point functions. It is obvious that

$$R_1 = \frac{g_2^3}{\sqrt{J}} \frac{1}{12} \sqrt{x(1-x)} [x^4 + (1-x)^4] \quad (27)$$

$$R_2 = \frac{g_2^3}{\sqrt{J}} \frac{1}{12} \sqrt{x(1-x)} \quad (28)$$

Notice the sum over operators in the first diagram of R_3 gives a integral $Jx \int_0^1 dy$. The vertices in the first diagram of R_3 are

$$\langle \bar{O}^J O^{xyJ} O^{(1-xy)J} \rangle = \frac{g_2}{\sqrt{J}} \sqrt{xy(1-xy)} \quad (29)$$

$$\langle \bar{O}^{xyJ} \bar{O}^{x(1-y)J} O^{xJ} \rangle = \frac{g_2}{\sqrt{J}} x^{\frac{3}{2}} \sqrt{y(1-y)} \quad (30)$$

$$\langle \bar{O}^{(1-xy)J} O^{x(1-y)J} O^{(1-x)J} \rangle = \frac{g_2}{\sqrt{J}} (1-xy)^{\frac{3}{2}} \left(\frac{1-x}{1-xy} \right)^{\frac{1}{2}} \left(\frac{x(1-y)}{1-xy} \right)^{\frac{1}{2}} \quad (31)$$

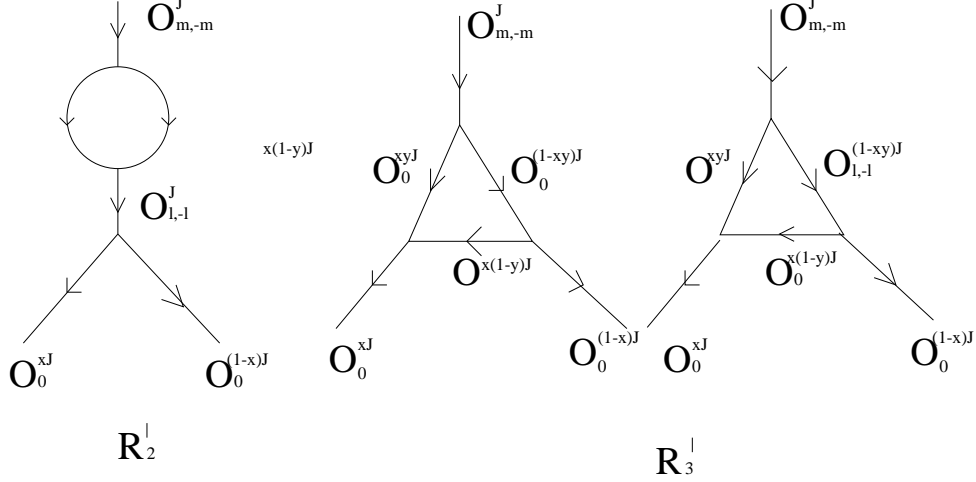


Figure 6: String theory diagrams contribute to $\langle \bar{O}_{m,-m}^J O_0^{J_1} O_0^{J_2} \rangle_{torus}$. Diagrams can be organized into 3 groups similar to those in figure 5. Here we only draw two groups which are different from figure 5. There are 4 diagrams in R'_3 . We only draw 2 of them. The other 2 diagrams is symmetric to what we draw by exchange of the 2 decayed operators.

So we find

$$\begin{aligned}
R_3 &= \int_0^1 J x dy \left(\frac{g_2}{\sqrt{J}} \sqrt{xy(1-xy)} \right) \left(\frac{g_2}{\sqrt{J}} x^{\frac{3}{2}} \sqrt{y(1-y)} \right) \left(\frac{g_2}{\sqrt{J}} (1-xy)^{\frac{3}{2}} \left(\frac{1-x}{1-xy} \right)^{\frac{1}{2}} \left(\frac{x(1-y)}{1-xy} \right)^{\frac{1}{2}} \right) \\
&+ (x \rightarrow (1-x)) \\
&= \frac{g_2^3}{\sqrt{J}} \frac{1}{12} \sqrt{x(1-x)} (x^3 + (1-x)^3 + x^3(1-x) + x(1-x)^3)
\end{aligned} \tag{32}$$

Now we can write R_1 , R_2 and R_3 in terms of Q_1 , Q_2 and Q_3 . We find

$$\begin{aligned}
R_1 &= 2Q_1 \\
R_2 &= 2Q_1 + 4Q_2 + 6Q_3 \\
R_3 &= 2Q_1 + 2Q_2
\end{aligned} \tag{33}$$

This is in agreement with equation (46). The total contribution to torus three point function is $Q_1 + Q_2 + Q_3$. In terms of R_1 , R_2 and R_3 it is

$$Q_1 + Q_2 + Q_3 = \frac{1}{6} (R_1 + R_2 + R_3) \tag{34}$$

Thus the symmetry factors of all diagrams in figure 5 are $\frac{1}{6}$.

Now we consider three point function with a BMN operator $\langle \bar{O}_{m,-m}^J O_0^{J_1} O_0^{J_2} \rangle_{torus}$. String theory diagrams contributing to this process are depicted in figure 6. Again we classify the diagrams by 3 groups and denote their contributions by R'_1 , R'_2 and

R'_3 . The calculation of R'_1 is the same as before. But in the case of R'_2 , we need to sum over all possible operators that is related to $O_{m,-m}^J$ by one loop propagation. The summation can be done by the summation formulae in appendix C.

$$R'_1 = \frac{g_2^3}{\sqrt{J}} \frac{1}{12} \left(-\frac{\sin^2(m\pi x)}{m^2\pi^2} \right) [x^4 + (1-x)^4] \quad (35)$$

$$\begin{aligned} R'_2 &= \sum_{l=-\infty}^{+\infty} 2 \langle \bar{O}_{m,-m}^J O_{l,-l}^J \rangle_{torus} \langle \bar{O}_{l,-l}^J O_0^{J_1} O_0^{J_2} \rangle_{planar} \\ &= \frac{g_2^3}{\sqrt{J}} \frac{1}{24m^6\pi^6} [-3 - (1+2x-2x^2)^2 m^4 \pi^4 + 3(3-2x+2x^2) m^2 \pi^2 \\ &\quad + (3-3(3-4x+4x^2) m^2 \pi^2 + (1-4x+6x^2-4x^3+2x^4) m^4 \pi^4) \cos(2m\pi x) \\ &\quad - (3(1-2x)m\pi + 4(-1+3x-3x^2+2x^3) m^3 \pi^3) \sin(2m\pi x)] \end{aligned} \quad (36)$$

The calculation of R'_3 involves two diagrams and their symmetric partners by exchanging of the two decayed operators. we also need to use the summation formulae in appendix C. The result of doing sum and integrals is

$$\begin{aligned} R'_3 &= \frac{g_2^3}{\sqrt{J}} \frac{1}{24m^6\pi^6} [12 + 12x(x-1) m^2 \pi^2 + (-1 + 6x^2 - 12x^3 + 6x^4) m^4 \pi^4 \\ &\quad + (-12 + 12x(x-1) m^2 \pi^2 + (1-4x+6x^2-4x^3+2x^4) m^4 \pi^4) \cos(2m\pi x) \\ &\quad + (12(1-2x)m\pi + 2(1-3x+3x^2-2x^3) m^3 \pi^3) \sin(2m\pi x)] \end{aligned} \quad (37)$$

Using equation (24), (25), (26), (35), (36) and (37) one readily check

$$\begin{aligned} R'_1 &= 2Q'_1 \\ R'_2 &= 2Q'_1 + 4Q'_2 + 6Q'_3 \\ R'_3 &= 2Q'_1 + 2Q'_2 \end{aligned} \quad (38)$$

And the total contribution to the torus three point function is

$$\langle \bar{O}_{m,-m}^J O_0^{J_1} O_0^{J_2} \rangle_{torus} = Q'_1 + Q'_2 + Q'_3 = \frac{1}{6} (R'_1 + R'_2 + R'_3) \quad (39)$$

Thus we have found the agreement between field theory and string theory calculations. It would be also interesting to do calculations in the case of three point functions involving two BMN operators such as $\langle \bar{O}_{m,-m}^J O_{n,-n}^{J_1} O^{J_2} \rangle_{torus}$.

4 Two loop string propagation

First we consider the vacuum operator $\langle \bar{O}^J O^J \rangle_{genus\ 2}$. The three diagrams S_1 , S_2 and S_3 are depicted in figure 7. S_1 and S_2 are directly related to torus two point function.

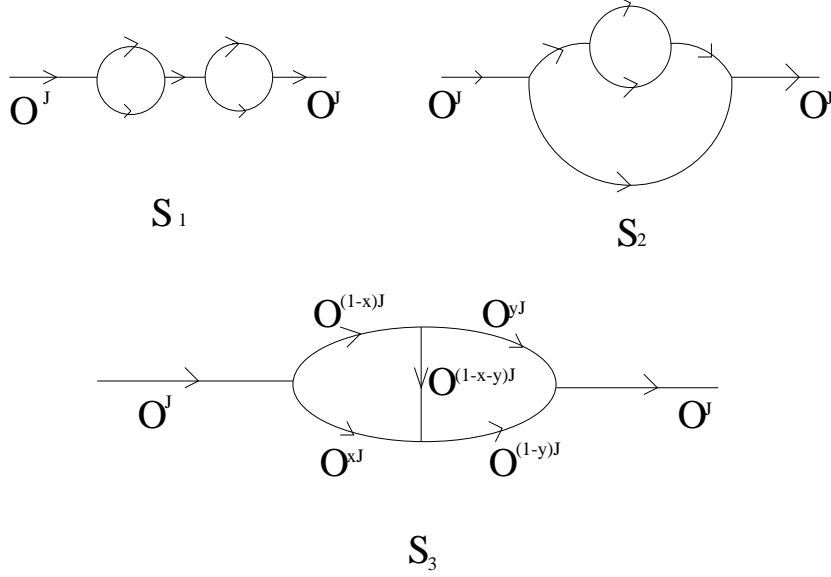


Figure 7: There are three diagrams contribute to $\langle \bar{O}^J O^J \rangle_{genus\ 2}$. S_1 and S_2 are unamputated diagrams while S_3 is a amputated diagram.

S_3 is a integral in the range of $x + y < 1$ as shown in the diagram. We calculate these diagrams

$$S_1 = \frac{1}{144} g_2^4 \quad (40)$$

$$\begin{aligned} S_2 &= g_2^4 \int_0^1 dx x(1-x) \frac{1}{12} x^4 \\ &= \frac{1}{504} g_2^4 \end{aligned} \quad (41)$$

$$\begin{aligned} S_3 &= g_2^4 \int_{0 < x, y, x+y < 1} dx dy x(1-x)y(1-y)(1-x-y) \\ &= \frac{1}{280} g_2^4 \end{aligned} \quad (42)$$

Suppose the symmetry factors of the three diagrams S_1 , S_2 and S_3 are a_1 , a_2 and a_3 , then from genus 2 two point function results in [5, 8] we will require

$$\frac{a_1}{144} + \frac{a_2}{504} + \frac{a_3}{280} = \frac{1}{5!2^4} \quad (43)$$

The genus 2 two point function of BMN operators are computed in [8]. It would be interesting to determine the symmetry factors by combinatorics argument as in appendix A or by analytic calculations of string theory diagrams and comparing with equation (C.36) in [8]. The string theory calculation of $\langle \bar{O}_{m,-m}^J O_{n,-n}^J \rangle_{genus\ 2}$

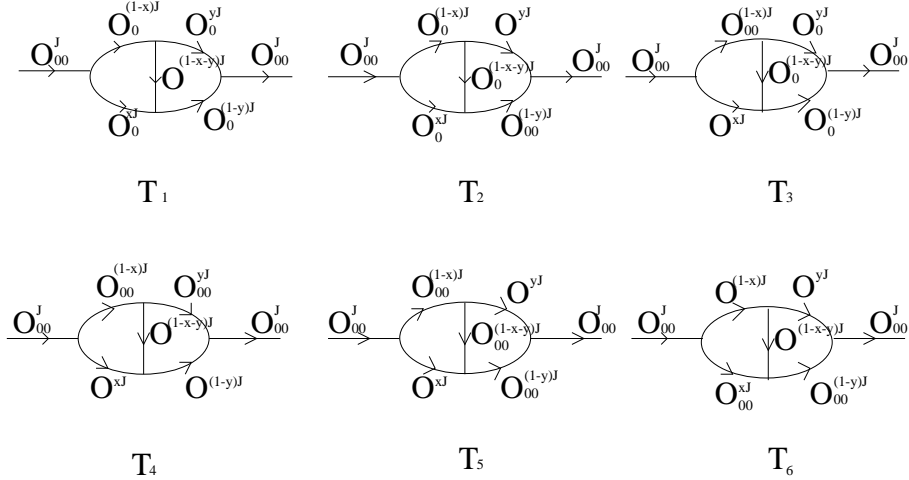


Figure 8: String theory diagrams of $\langle \bar{O}_{00}^J O_{00}^J \rangle_{genus\ 2}$. We only draw amputated diagrams since unamputated diagrams are the same as in figure 7. Notice diagrams T_2 and T_3 , T_4 and T_6 are equal by symmetry. Also diagrams T_1 , T_2 and T_3 need to be multiplied by a factor of 2 since there are two ways to separate the two different scalar insertions. Interestingly, the sum of all these 6 diagrams give the same result as a single diagram S_3 in the figure 7, as expected from analytic results of [5, 8].

will involve 6 amputated diagrams. In cases of $m = n = 0$ or $m = 0, n \neq 0$ the diagrams are easy to calculate. For $m = n = 0$ the sum of the six diagrams in figure 8 interestingly gives the same result as a single diagram S_3 . The readers can easily check (note diagrams T_1, T_2 and T_3 have double contributions)

$$2T_1 + 2T_2 + 2T_3 + T_4 + T_5 + T_6 = S_3 \quad (44)$$

This is expected since higher genus contributions to the correlators of chiral operators are the same regardless of the number of supergravity excitations [5, 8]. In the appendix B we compute the case $m = 0, n \neq 0$ and find all diagrams cancel, as expected from the genus 2 two point function equation (C.36) in [8].

5 Conclusion

In this paper we have described string interaction in pp-wave from $\mathcal{N} = 4$ super Yang Mills. From our proposal we can effectively compute the free field correlation functions of BMN operators to arbitrary genus by diagrammatic expansion in terms of free planar three point functions. It would be interesting to perform more detailed calculations as pointed out in the text or try to give a general analytic proof of these mathematical identities at arbitrary genus. It is also interesting to generalize the results to interacting field theory. In this case the Yang Mills theory is perturbative

in two parameters λ' and g_2 and there are complications of operator mixing and redefining in this double scaling limit [5, 8]. One will need to represent the cubic string vertex with interacting planar three point functions instead of the free planar three point functions we used. The planar three point functions in the first order expansion of λ' have been computed in [14]. It would be interesting to use their results to do the calculations and compare with non-planar contributions to correlators in interacting Yang Mills theory. But we should caution the readers the relation between three point vertex in field theory and string theory is still unclear at nonzero λ' [17]. The three point vertex in pp-wave light cone string field theory is a very complicated smoothly interpolating function which involves fractional powers in small λ' expansion [10, 17].

The natural question to ask is what we are really doing here. Can we interpret the discovered identities as consequences of pp-wave/CFT correspondence, or are they just mathematical coincidence and possibly related to some unknown properties of field theory itself? The answer is not convincingly clear at this point although we have been inclined to the former explanation. One possible interpretation is wave function renormalization. While the authors in [8] computed energy correction, what we did in section 2 looks like wave function renormalization in quantum mechanics.⁵ Remember in quantum perturbation theory the first order wave function renormalization is

$$\langle n|n \rangle = 1 + \sum_{k \neq n} \frac{|V_{kn}|^2}{(E_n - E_k)^2} \quad (45)$$

In string field theory the matrix elements contain a prefactor which exactly cancels $(E_n - E_k)^2$ in the denominator [8]. That is why we never need to use energies in our calculation. But in this framework it is hard to explain the factor of $\frac{1}{2}$ there and all other calculations in section 3 and section 4 besides the fact that we don't know why the free torus two point function should correspond to wave function renormalization on the string theory side. Despite lack of interpretations, our calculations nevertheless set up computational rules to get the right answer and indeed point out a clear correspondence on both sides. Our calculations may help to better understand of the question of holography, which has been address in previous works [6, 25, 26]. But this question is still unclear. We do not yet have a clear prescription of what is the correspondence between the bulk and boundary as we did in the context of AdS/CFT (by Witten diagram) . Our calculations would provide some sense as to what specifically do we need to compare on both sides. It would be interesting to further study this question.

Acknowledgments

We thank Vijay Balasubramanian and Asad Naqvi for collaborations at early stage of the project and for readings of the manuscript. We are also grateful to Thomas S. Levi, Gary Shiu and Matt Strassler for illuminating discussions.

⁵We thank Asad Naqvi for pointing out this to us.

A Derivation of symmetry factors

In this appendix we give a practical prescription for deriving symmetry factors of string theory diagrams we computed. We have considered two cases of one loop propagation diagrams and one loop cubic diagrams where the countings are relatively simple (For two point functions at genus 2 level we would need to count 21 field theory diagrams [8]).

A.1 one loop propagation diagrams

We denote a close string with n segments by $(a_1 a_2 \cdots a_n)$, where the string are regarded as the same by cyclic rotation. For example, $(a_1 a_2 \cdots a_n)$ and $(a_2 a_3 \cdots a_n a_1)$ are the same string. We denote the processes of string splitting and joining by $(a_1 a_2 \cdots a_n) \rightarrow (a_1 a_2 \cdots a_i)(a_{i+1} \cdots a_n)$ and $(a_1 a_2 \cdots a_i)(a_{i+1} \cdots a_n) \rightarrow (a_1 a_2 \cdots a_n)$. Now imagine figure 3 as a string of 4 segments goes from (1234) to (2143). How many ways can we do this with our rules? A little counting reveal that at one loop level there are only two processes as the following

$$(1234) \rightarrow (12)(34) \rightarrow (2143)$$

$$(1234) \rightarrow (23)(41) \rightarrow (2143)$$

Here since (12) and (21), (34) and (43) are the same, we can join (12)(34) in to (2143). These two processes are exactly one loop string propagation diagrams in figure 2. Thus we conclude we have overcounted by a factor of 2 when we do string theory diagram calculations. This explain the symmetry factor of $\frac{1}{2}$ in equation (17). At this point the meaning of the procedure may be a little unclear to the readers. The validity of this procedure will be justified by a less trivial example of one loop cubic diagrams in the next subsection, in which we find precise agreements with direct field theory and string theory diagrams calculation.

A.2 one loop cubic diagrams

Now we consider field theory diagrams in figure 4. Diagrams Q_1 , Q_2 and Q_3 represent the processes $(123456) \rightarrow (14325)(6)$, $(36)(1542)$, $(153)(426)$. How many ways can we go from initial state to final states? For Q_1 , there are six processes

1. $(123456) \rightarrow (23)(4561) \rightarrow (325614) \rightarrow (14325)(6)$
2. $(123456) \rightarrow (34)(5612) \rightarrow (432561) \rightarrow (14325)(6)$
3. $(123456) \rightarrow (12345)(6) \rightarrow (23)(451)(6) \rightarrow (51432)(6)$
4. $(123456) \rightarrow (12345)(6) \rightarrow (34)(512)(6) \rightarrow (43251)(6)$
5. $(123456) \rightarrow (34)(5612) \rightarrow (34)(125)(6) \rightarrow (43251)(6)$
6. $(123456) \rightarrow (23)(4561) \rightarrow (23)(145)(6) \rightarrow (51432)(6)$

As we track the string splitting and joining processes and compare with string theory diagrams in figure 5, we find process 1,2 belong to type R_2 string theory diagrams; process 3,4 belong to type R_1 string theory diagrams; process 5,6 belong to type R_3 string theory diagrams. For Q_2 all possible processes are

1. $(123456) \rightarrow (234)(156) \rightarrow (423615) \rightarrow (36)(4215)$
2. $(123456) \rightarrow (234)(156) \rightarrow (342156) \rightarrow (36)(4215)$
3. $(123456) \rightarrow (12)(3456) \rightarrow (215634) \rightarrow (63)(2154)$
4. $(123456) \rightarrow (12)(3456) \rightarrow (12)(45)(36) \rightarrow (36)(2154)$
5. $(123456) \rightarrow (45)(1236) \rightarrow (542361) \rightarrow (36)(5421)$
6. $(123456) \rightarrow (45)(1236) \rightarrow (45)(12)(36) \rightarrow (36)(5421)$

Here process 1,2,3,5 belong to type R_2 string theory diagrams; process 4,6 belong to type R_3 string theory diagram. For Q_3 all possible processes are

1. $(123456) \rightarrow (123)(456) \rightarrow (312645) \rightarrow (531)(264)$
2. $(123456) \rightarrow (123)(456) \rightarrow (231564) \rightarrow (315)(264)$
3. $(123456) \rightarrow (234)(561) \rightarrow (342615) \rightarrow (315)(426)$
4. $(123456) \rightarrow (234)(561) \rightarrow (423156) \rightarrow (315)(426)$
5. $(123456) \rightarrow (345)(126) \rightarrow (534261) \rightarrow (531)(426)$
6. $(123456) \rightarrow (345)(126) \rightarrow (453126) \rightarrow (531)(426)$

All processes belong to type R_2 string theory diagrams. Summarizing our results, type R_1 diagrams have 2 contributions from Q_1 ; type R_2 diagrams have 2 contributions from Q_1 , 4 contributions from Q_2 , 6 contributions from Q_3 ; type R_3 diagrams have 2 contributions from Q_1 , 2 contributions from Q_2 . So we conclude

$$\begin{aligned}
R_1 &= 2Q_1 \\
R_2 &= 2Q_1 + 4Q_2 + 6Q_3 \\
R_3 &= 2Q_1 + 2Q_2
\end{aligned} \tag{46}$$

This is in exact agreements with equation (33) and (38).

B Cancellation for chiral/non-chiral amplitude

From [8] we know the two point function of a chiral operator with a non-chiral BMN operator vanishes at genus 1 and 2 level. The planar three point functions $\langle \bar{O}_{00}^J O_{n,-n}^{J_1} O^{J_2} \rangle$ also vanish. We expect it is generally true that a chiral state can not propagate or decay into non-chiral states at arbitrary higher genus. In this appendix we verify $\langle \bar{O}_{00}^J O_{n,-n}^J \rangle_{genus\ 2} = 0$ and $\langle \bar{O}_{00}^J O_{n,-n}^{J_1} O^{J_2} \rangle_{torus} = 0$ from string theory calculations. Knowing $\langle \bar{O}_{00}^J O_{n,-n}^J \rangle_{torus} = 0$ and $\langle \bar{O}_{00}^J O_{n,-n}^{J_1} O^{J_2} \rangle_{planar} = 0$, we only need to consider amputated diagrams and show they cancel.

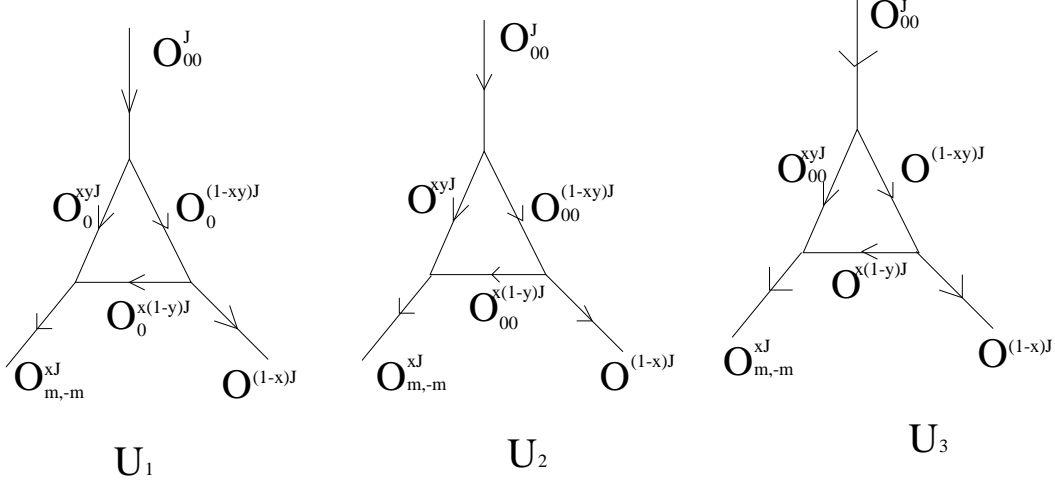


Figure 9: There are three amputated diagrams of $\langle \bar{O}_{00}^J O_{m,-m}^{J_1} O^{J_2} \rangle_{torus}$. Note the first diagram U_1 has double contribution since there are two ways to separate the two scalar excitations. Calculations show the three diagrams exactly cancel each other.

B.1 One loop cubic string interaction

The diagrams are depicted in figure 9. Calculations show

$$2U_1 = -2 \frac{g_2^3}{\sqrt{J}} x^{\frac{9}{2}} (1-x)^{\frac{1}{2}} \int_0^1 dy y(1-y)(1-xy) \frac{\sin^2(m\pi y)}{m^2 \pi^2} \quad (47)$$

$$U_2 = U_3 = \frac{g_2^3}{\sqrt{J}} x^{\frac{9}{2}} (1-x)^{\frac{1}{2}} \int_0^1 dy y(1-y)(1-xy) \frac{\sin^2(m\pi y)}{m^2 \pi^2} \quad (48)$$

Without doing the integral, we can see the contributions of the three diagrams cancel $2U_1 + U_2 + U_3 = 0$.

B.2 Two loop string propagation

The relevant diagrams are depicted in figure 10. As usual we calculate these diagrams. For example

$$V_1 = g_2^4 \int_{0 < x, y, x+y < 1} dx dy x^2 (1-x) y (1-x-y) \left(-\frac{\sin^2(n\pi y)}{n^2 \pi^2} \right) \quad (49)$$

Note diagrams V_1 , V_2 and V_3 have double contributions. We leave the readers to check $2V_1 + 2V_2 + 2V_3 + V_4 + V_5 + V_6 = 0$. The calculation is simple since the cancellation occurs without doing the sum and the integral.

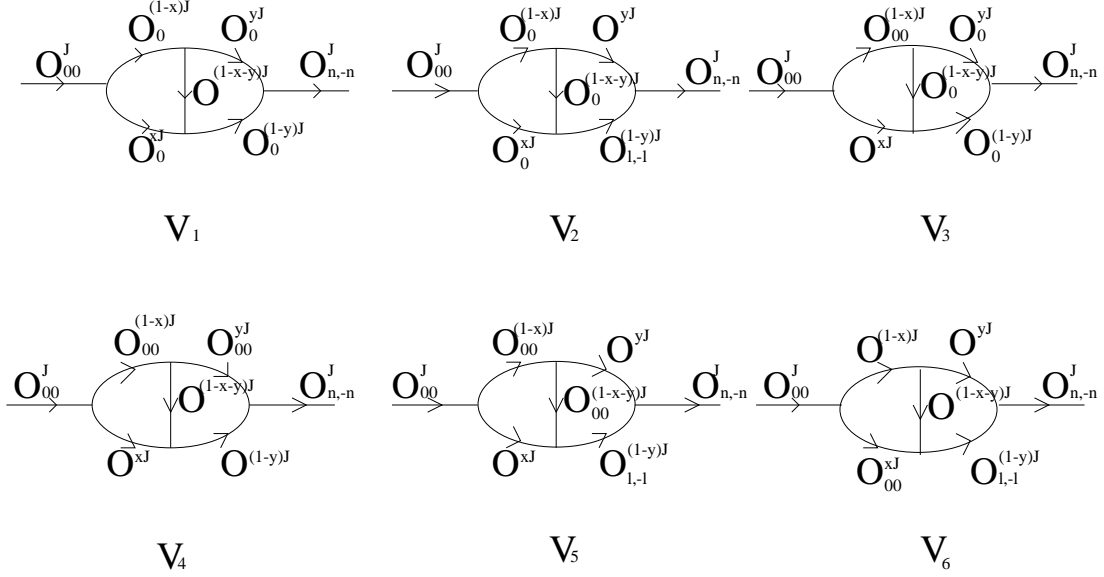


Figure 10: Similar to figure 8, there are 6 diagrams contribute to $\langle \bar{O}_{00}^J O_{n,-n}^J \rangle_{\text{genus } 2}$. Again we note diagrams V_1 , V_2 and V_3 have double contributions.

C Some summation formulae

We will need to use some useful summation formulae when we sum over all operators in the string theory loop diagram. Note the useful identity in [27] (see also appendix D of [24])

$$\sum_{l=-\infty}^{\infty} (-1)^l \frac{e^{ily}}{l + \alpha} = \frac{\pi}{\sin(\pi\alpha)} e^{-i\alpha y}, \quad -\pi < y < \pi \quad (50)$$

From this equation we can derive (for $0 < \beta < 1$)

$$\sum_{p \neq 0, p=-\infty}^{\infty} \frac{\sin^2(p\pi\beta)}{(p - \alpha_1)(p - \alpha_2)} = \frac{\pi}{(\alpha_1 - \alpha_2)} \left[\frac{\sin(\alpha_1\pi(1 - \beta)) \sin(\alpha_1\pi\beta)}{\sin(\alpha_1\pi)} - \frac{\sin(\alpha_2\pi(1 - \beta)) \sin(\alpha_2\pi\beta)}{\sin(\alpha_2\pi)} \right] \quad (51)$$

Then we can take the derivatives of α_1 and α_2 and take specific limits of α_1 and α_2 on both sides of the equation. Here are some specific identities that will be useful for our calculations (Assuming m is an integer and α is not an integer).

$$\sum_{p \neq 0} \frac{\sin^2(\beta p \pi)}{(p - \alpha)^2 p^2} = -\frac{2\pi \sin(\alpha\pi(1 - \beta)) \sin(\alpha\pi\beta)}{\alpha^3 \sin(\alpha\pi)} \quad (52)$$

$$+ \frac{\pi^2}{\alpha^2} \left[\frac{(1 - \beta) \sin^2(\alpha\pi\beta) + \beta \sin^2(\alpha\pi(1 - \beta))}{\sin^2(\alpha\pi)} + \beta(1 - \beta) \right]$$

$$\sum_{p \neq 0, p \neq m} \frac{\sin^2(\beta p \pi)}{(p-m)^2 p^2} = \frac{1}{6m^4} [-18 \sin^2(\beta m \pi) + (-1 + 6\beta - 6\beta^2)m^2 \pi^2 \cos(2\beta m \pi) + (1 + 6\beta - 6\beta^2)m^2 \pi^2 - 6(1 - 2\beta)m \pi \sin(2\beta m \pi)]$$

$$\sum_{p \neq 0, p \neq m} \frac{\sin^2(\beta p \pi)}{(p-m)^2 p^3} = \frac{1}{6m^5} [-36 \sin^2(\beta m \pi) + (-1 + 6\beta - 6\beta^2)m^2 \pi^2 \cos(2\beta m \pi) + (1 + 12\beta - 12\beta^2)m^2 \pi^2 - 9(1 - 2\beta)m \pi \sin(2\beta m \pi)]$$

$$\sum_{p \neq 0, p \neq m} \frac{\sin^2(\beta p \pi)}{(p-m)^2 p^4} = \frac{1}{6m^6} [-60 \sin^2(\beta m \pi) + (-1 + 6\beta - 6\beta^2)m^2 \pi^2 \cos(2\beta m \pi) + (1 + 18\beta - 18\beta^2 + 2\beta^2(1 - \beta)^2 m^2 \pi^2)m^2 \pi^2 - 12(1 - 2\beta)m \pi \sin(2\beta m \pi)]$$

$$\sum_{p \neq 0, p \neq m} \frac{\sin^2(\beta p \pi)}{(p-m)^4 p^2} = \frac{1}{90m^6} \{-225 + 45m^2 \pi^2 + 90\beta(1 - \beta)m^2 \pi^2 + m^4 \pi^4 + [225 - 45(1 - 6\beta + 6\beta^2)m^2 \pi^2 + (-1 + 30\beta^2 - 60\beta^3 + 30\beta^4)m^4 \pi^4] \cos(2\beta m \pi) + 60(1 - 2\beta)(-3 - \beta m^2 \pi^2 + \beta^2 m^2 \pi^2)m \pi \sin(2\beta m \pi)\}$$

References

- [1] J. Maldacena, “The Large N limit of superconformal field theories and supergravity,” *Adv. Theor. Math. Phys.* **2** (1998) 231, [hep-th/9711200](#); S. S. Gubser, I. R. Klebanov, and A. M. Polyakov, “Gauge theory correlators from noncritical string theory,” *Phys. Lett.* **B428** (1998) 105, [hep-th/9802109](#); E. Witten, “Anti-de Sitter space and holography,” *Adv. Theor. Math. Phys.* **2** (1998) 253, [hep-th/9802150](#).
- [2] D. Berenstein, J. Maldacena and H. Nastase, “Strings in flat space and pp waves from N = 4 super Yang Mills,” [hep-th/0202021](#).
- [3] M. Blau, J. Figueroa-O’Farrill, C. Hull and G. Papadopoulos, “A new maximally supersymmetric background of IIB superstring theory,” *JHEP* **0201**, 047 (2002) [[arXiv:hep-th/0110242](#)]; M. Blau, J. Figueroa-O’Farrill, C. Hull and G. Papadopoulos, “Penrose limits and maximal supersymmetry,” [arXiv:hep-th/0201081](#).
- [4] R. R. Metsaev, “Type IIB Green-Schwarz superstring in plane wave Ramond-Ramond background,” *Nucl. Phys. B* **625**, 70 (2002)

- [arXiv:hep-th/0112044]; R. R. Metsaev and A. A. Tseytlin, “Exactly solvable model of superstring in plane wave Ramond-Ramond background,” arXiv:hep-th/0202109.
- [5] C. Kristjansen, J. Plefka, G. W. Semenoff, and M. Staudacher, “A New double-scaling limit of N=4 super Yang-Mills theory and pp-wave strings,” hep-th/0205033.
- [6] D. Berenstein and H. Nastase, “On lightcone string field theory from super Yang-Mills and holography,” hep-th/0205048.
- [7] D.J. Gross, A. Mikhailov, and R. Roiban, “Operators with large R charge in N=4 Yang-Mills theory,” hep-th/0205066;
A. Santambrogio and D. Zanon, “Exact anomalous dimensions of N=4 Yang-Mills operators with large R charge,” hep-th/0206079.
- [8] N.R. Constable, D.Z. Freedman, M. Headrick, S. Minwalla, L. Motl, A. Postnikov, and W. Skiba, “PP-wave string interactions from perturbative Yang-Mills theory,” hep-th/0205089.
- [9] M. Spradlin and A. Volovich, “Superstring interactions in a pp-wave background,” hep-th/0204146.
- [10] M. Spradlin and A. Volovich, “Superstring interactions in a pp-wave background II,” hep-th/0206073.
- [11] R. Gopakumar, “String Interactions in PP-waves,” hep-th/0205174;
H. Verlinde, “Bits, matrices and $1/N$,” hep-th/0206059.
- [12] Y. Kiem, Y. Kim, S. Lee and J. Park, “PP-wave/Yang-Mills Correspondence: An explicit check,” hep-th/0205279.
- [13] M. Huang, “Three point functions of N=4 super Yang Mills from light cone string field theory in pp-wave,” hep-th/0205311.
- [14] C. Chu, V.V. Khoze, G. Travaglini, “Three-point functions in N=4 super Yang-Mills theory and pp-wave ,” hep-th/0206005.
- [15] P. Lee, S. Moriyama and J.w. Park, “Cubic Interactions in PP-wave light cone string field theory ,” hep-th/0206065.
- [16] C. Chu, V.V. Khoze, G. Travaglini, “PP-wave string interactions from n-point correlators of BMN operators ,” hep-th/0206167.
- [17] I. R. Klebanov, M. Spradlin, A. Volovich, “New Effects in Gauge Theory from pp-wave Superstrings,” hep-th/0206221.

- [18] V. Balasubramanian, M. Berkooz, A. Naqvi and M. J. Strassler, “Giant gravitons in conformal field theory,” JHEP **0204**, 034 (2002), hep-th/0107119.
- [19] S. Corley, A. Jevicki and S. Ramgoolam, “Exact correlators of giant gravitons from dual $N = 4$ SYM theory,” hep-th/0111222.
- [20] R.C. Myers, “Dielectric-Branes,” JHEP 9912 (1999) 022, hep-th/9910053
- [21] J. McGreevy, L. Susskind, and N. Toumbas, “Invasion of the Giant Gravitons from Anti-de Sitter Space,” JHEP 0006 (2000) 008, hep-th/0003075
- [22] V. Balasubramanian, M. x. Huang, T. S. Levi and A. Naqvi, “Open strings from $N = 4$ super Yang-Mills,” hep-th/0204196.
- [23] L. Motl, “Proposals on nonperturbative superstring interactions,” hep-th/9701025;
T. Banks and N. Seiberg, “Strings from matrices,” Nucl. Phys. B **497**, 41(1997), hep-th/9702187;
R. Dijkgraaf, E. Verlinde and H. Verlinde, “Matrix string theory,” Nucl. Phys. B **500**, 43(1997), hep-th/9703030.
- [24] M. Green and J. Schwarz, “Superstring Interactions,” Nucl. Phys. B **218** (1983) 43.
- [25] S. R. Das, C. Gomez and S. J. Rey, “Penrose limit, spontaneous symmetry breaking and holography in pp-wave background,” hep-th/0203164;
E. Kiritsis and B. Pioline, “Strings in homogeneous gravitational waves and null holography,” hep-th/0204004;
R. G. Leigh, K. Okuyama and M. Rozali, “PP-waves and holography,” hep-th/0204026.
- [26] G. Siopsis, “Holography in the Penrose limit of AdS space,” hep-th/0205302;
S. R. Das, C. Gomez, “Realization of conformal and Heisenberg algebras in pp-wave-CFT correspondence,” hep-th/0206062.
- [27] E. Cremmer and J-L. Gervais, “Combining And Splitting Relativistic Strings,” Nucl. Phys. B **76** (1974) 209; “Infinite Component Field Theory Of Interacting Relativistic Strings And Dual Theory,” Nucl. Phys. B **90** (1975) 410.
- [28] W. Taylor, “Perturbative diagrams in string field theory,” arXiv:hep-th/0207132.